CHAPTER V

EFFECT OF INTERNAL BUBBLE SHAPES ON DIELECTRIC BEHAVIORS IN POLY(VINYLIDENE FLUORIDE) (PVDF) FILMS BY AZDC CHEMICAL BLOWING AGENT

5.1 Abstract

The porous PVDF films with regular spherical bubbles shape were produced by azodicabonamide (AZDC) compression molding technique, Yamada model was confirmed the connectivity of composites belonging to 0-3 type. This work highlighted the effect of bubbles shape (spherical and ellipsoidal shapes) on dielectric properties. The porous films were uniaxially stretched for ellipsoidal shape. The results reveals that the dielectric properties of the ellipsoidal shape are nearly stable than spherical shape with frequency range of 1 kHz – 10 MHz. Moreover, the non-cellular structure presents higher dielectric constant than cellular structure.

Keywords: Poly (vinylidenefluoride); PVDF foam; AZDC blowing agent; Compression molding; Dielectric Materials; Bubble Shapes

5.2 Introduction

In recent year, polymeric foams are found in wide applications when good mechanical properties and reduced density need to be coupled as is the case, for example, of acoustic insulation and damping, thermal insulation, and impact resistance [Throne, J.L. (1996),Gibson, L.J. and Ashby, M.F. (1988)]. The large and increasing volume of foamed materials has stimulated interests in developing innovations related to piezoelectric and dielectric materials that can be utilized in those applications [Klempner, D.(2004)].

Poly(vinylidiene fluoride) (PVDF) is a semi-crystalline thermoplastic that has superior chemical resistance properties. PVDF have been popular candidates for use as piezoelectric materials [H. Kawai (1969), S.B. Lang. (1993), H.S. Nalwa.(1991)]. These materials are known to display high piezoelectricity especially after conditioning by

applying high poling fields at raised temperatures. These favorable features give it wide applications in underwater flexible applications that need to have a light weight or density same as water. So, chemical blowing agents (CBAs) are used for foaming materials. The CBAs is solid organic compounds that release nitrogen gas at a specific processing temperature called "azo-compounds" are widely used, due to other CBAs as "Sodium bicarbonate" releases carbon dioxide, but the reaction also produces water which can cause rust on steel moulds. So, azodicabonamide (AZDC) are more interesting which have a decomposition temperature of 200-210°C which can be reduced to 189-200°C by means of metal compounds such as lead and zinc stabilizer [John Murphy (1996)].

This work was focused on internal bubble shape effect on dielectric properties.The chemical blowing agent was used to induce the internal bubble in PVDF film. So, the spherical bubble was created inside PVDF films by AZDC chemical blowing agent compression molding technique. Thus, the bubble-shape was changed to ellipsoid by stretching porous films. Subsequently, morphology of porous PVDF films was observed using optical microscope (OM). The dielectric constant and the loss tangent of porous PVDF films were measured as a function of frequency range of 1 kHz-10 MHz at room temperature by impedance/gain-phase analyzer in different % porosity, and bubbles shapes. Several criterias to improve foamability of PVDF polymers such as effect of processing, blowing agent, use of additives, are herein discussed.

5.3 Experimental

A. Materials

The PVDF powder used was manufactured from Solvay Company (Belgium) (Solef 1008). The chemical blowing agent as Azodicabonamide (AZDC) from Usaco (Thailand) Limited was used for creating bubbles. Also, ZnO (kicker agent) and all chemicals are used without further purification.

B. Preparation of Porous PVDF films

The dried AZDC chemical blowing agent was ground to powder and screened through a mesh #325. Thus the AZDC and PVDF powder could be homogeneously blended brabender which rotor speed 50 rpm and temperature 190°C in 30 min or until torque graph in computer show the constant. Finally, a mixed powder was put on the mold and placed in compression molding machine, the temperature of which was pre-set at 200°C for 5 min. Pressing the mould by 15 tons after a 5 min holding period, the mould was cooled to room temperature, and used for further measurements and characterizations

C. Preparation for Dielectric and Piezoelectric constant

The ellipsoidal shape of internal bubble can be obtained by stretching with Universal Testing Machine (LLOYD LRX) and Heater Chamber in Figure 5.1. Then, generate an electric displacement and store the electric charge, the poling with an DC electric field of 50 kV/mm.

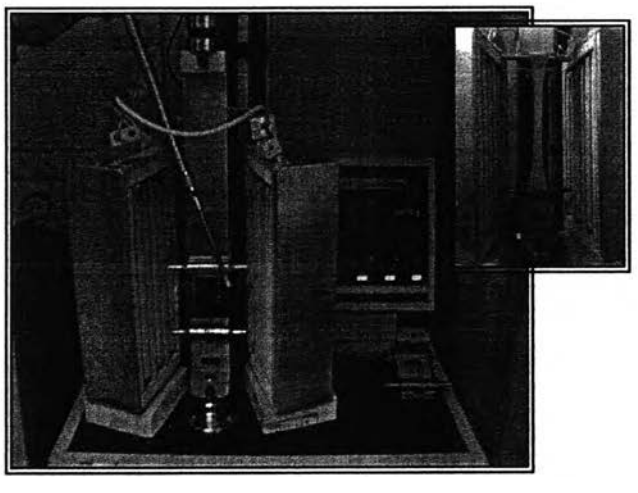

Figure 5.1 Assembly of thermal cabinet equipment for stretching PVDF films.

D. Characterizations

The distribution of bubbles and morphological characterization were performed using Optical Microscope research stereo (model SZH 10, OLYMPUS). The XRD measurements (Rigaku, model Dmax 2002) were carried out at 40 kV and 30mA with Cu K radiation for characterization phase and structure in PVDF. The heat capacity of the composite, which reflects the ability of the composite to store heat, was analyzed using a Differential Scanning Calorimeter (Perkin Elmer, DSC7). Finally, the dielectric constant and dielectric loss of the composite were characterized by using the LCR meter (Hewlett Packard., model 4194A).

5.4 Results and Discussion

A. Physical Properties

The compression molding technique can be produced porous PVDF films thickness of 0.569-0.684 mm as shown in Figure 5.2. Also, compressed film showed a non-cellular structure which each bubbles far apart from others and a smooth microstructure representing stronger properties. Moreover, the induced bubbles shapes film this technique are much regular than those from phase inversion technique.

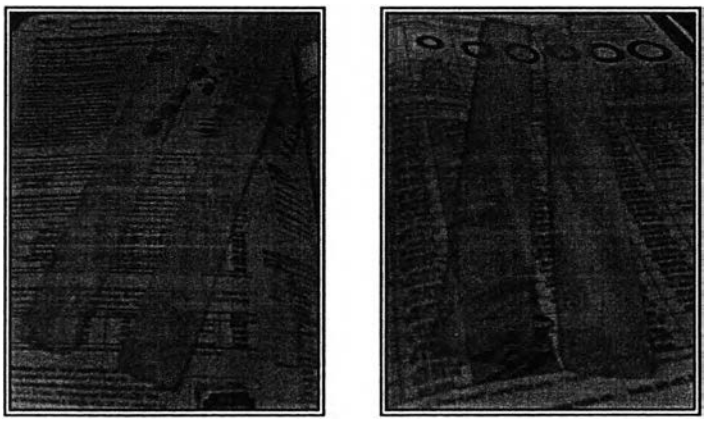

Figure 5.2 Porous PVDF films by AZDC compression molding technique.

5.4.1 Optical Microscope (OM)

a) Effect of ZnO (kicker agent)

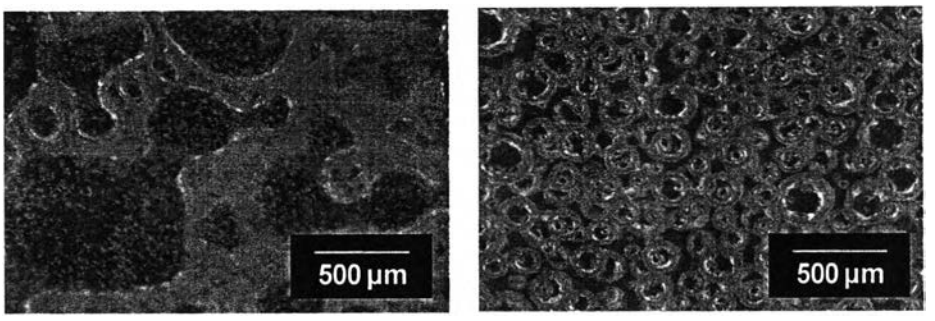

(a) **(b)**

Figure 5.3 PVDF Foam by (a) adding and (b) non-adding ZnO.

Optical micrographs show the cellular structure of the corresponding foams. Actually, the AZDC releases gases at high temperature up to 200-212°C. The adding of ZnO, which is act as kicker agent, will activate the AZDC to releases gases at lower temperature 180-200°C and found that the amount of ZnO usage is effect on irregulars size and shape as shown in Figure 5.3. Due to PVDF have a T_m 180°C nearly decomposition temperature of AZDC, ZnO can not used in this work.

b) Effect of Mixing (Internal and External)

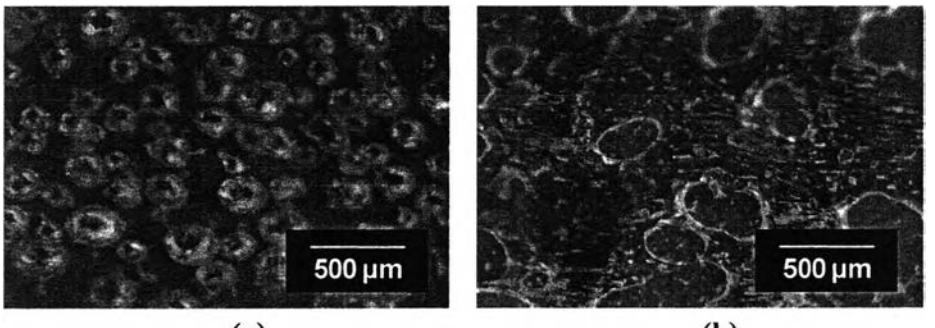

(a) **(b)**

Figure 5.4 Mixing between PVDF and AZDC by (a) internal and (b) external mixing.

In Figure 5.4, it can be noted that internal mixing provides approximately the same dimension of cells more than external mixing. Because the internal mixing of AZDC in PVDF powder can be yielded more regular a distribution and a dispersion than external mixing.

c) Effect of Azodicabonamide (AZDC) Concentrations (phr)

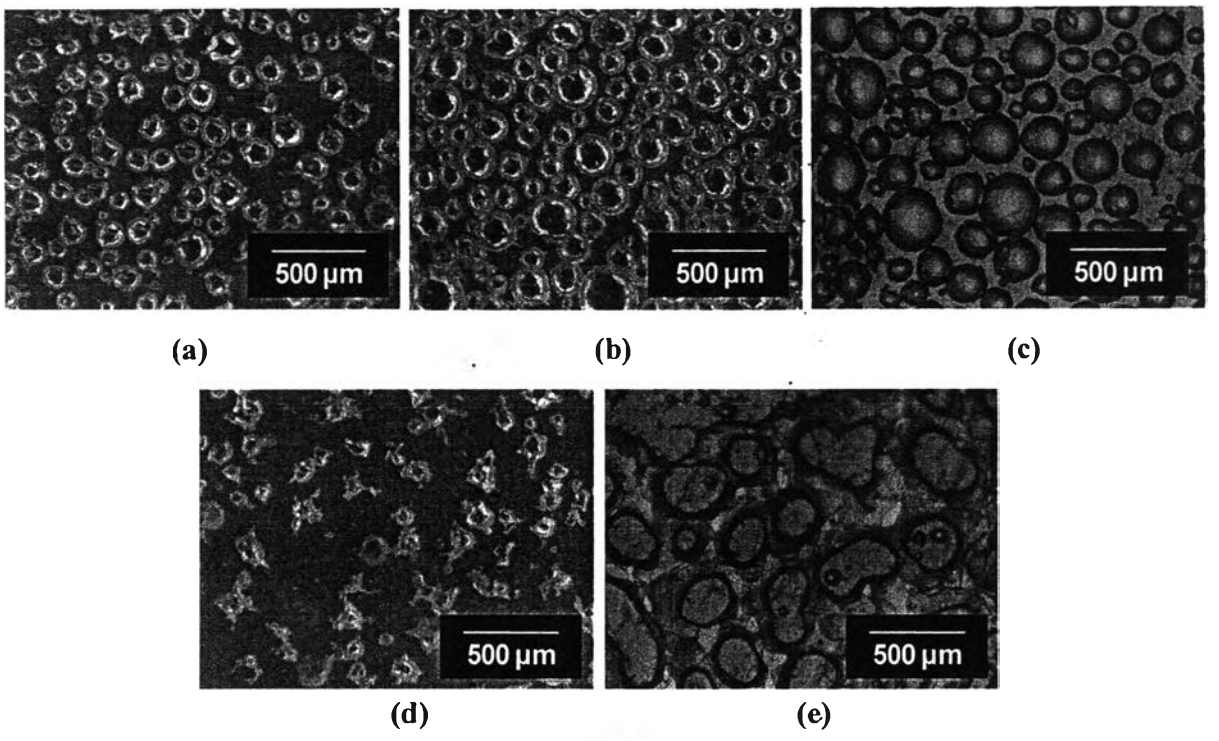

Figure 5.5 The effect of chemical blowing agent on foam density of PVDF films from optical microscopy (a) 0.03%,(b) 0.3%, (c) 3% , (d) 0.01% (minimum) and (e) 7% (maximum) (phr).

In Figure 5.5, the optical micrographs show the different amount bubbles inside PVDF films. It can be noted that samples AZDC contain in fraction of 0.03, 0.3, 3%, 0.01% and 7% (phr) have different pore size and density but approximately the same bubble dimension as a spherical shape. When adding excess AZDC, the bubbles was agglomerated become a larger irregular bubble. Nevertheless, this technique has higher uniform shape than phase inversion technique.

The effect of bubbles shapes on dielectric behavior in porous PVDF films was studied in this work; the films were stretching (1:1) by UTM machine in chamber 90°C. Thus, the bubbles in spherical and ellipsoidal shapes were confirmed by optical micrograph images as shown in Figure 5.6.

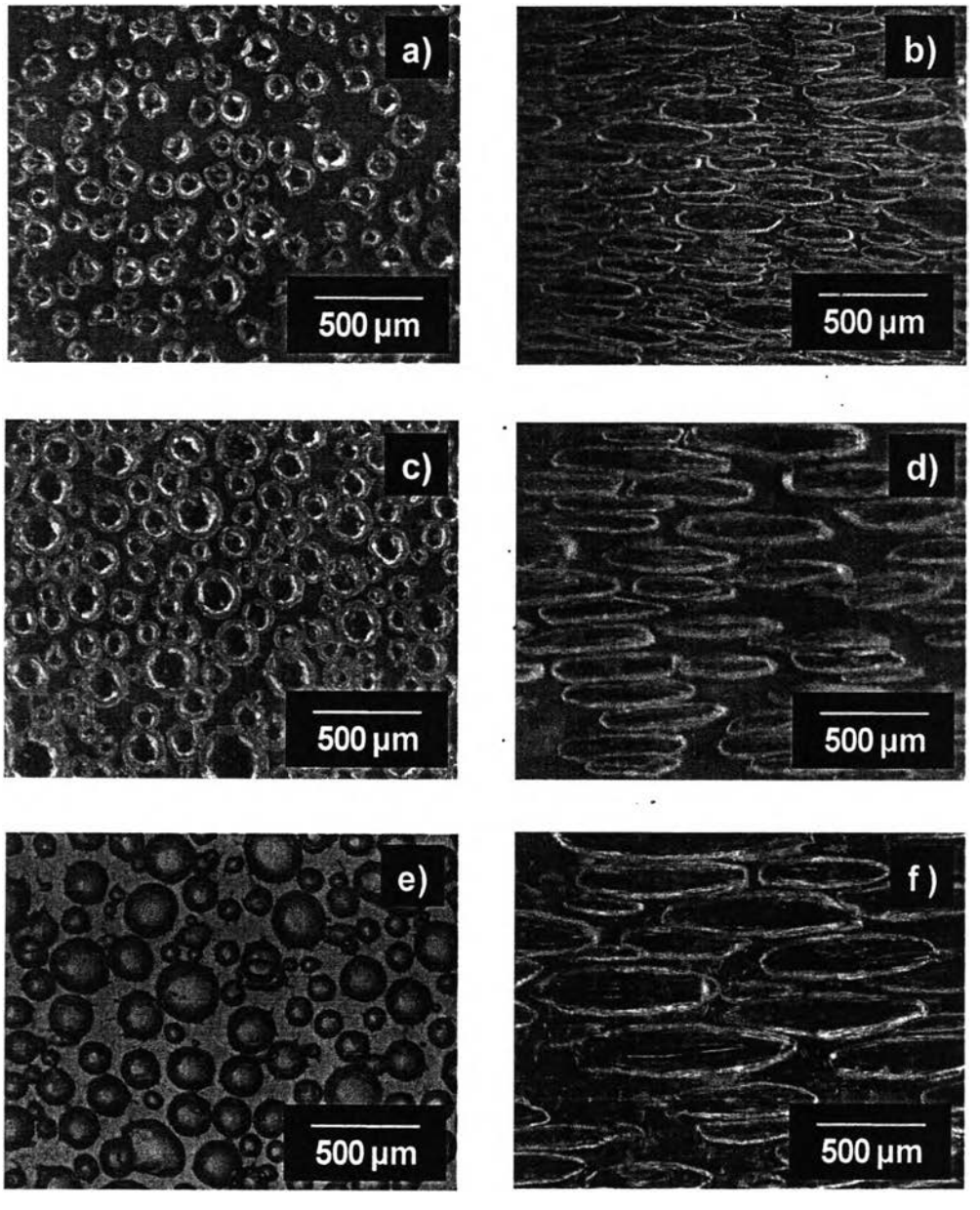

Figure 5.6 The optical micrograph of spherical shape at (a) 0.03, (c) 0.3, (e) 3% and ellipsoidal shape at (b) 0.03, (d) 0.3, (f) 3% of AZDC in PVDF films

5.4.2 Density of Porous films

The apparent densities of porous PVDF film are measured by Pycnometer (Quantachrome, Ultrapycnometer 1000 Version 2.4)

Table 5.1 The Comparison between Density of Non-porous and Porous PVDF film

Sample	Average Density(g/cc)
Non-porous PVDF films	1.7894
AZDC in range 0.01-0.05 % (phr)	1.3678-1.4093
AZDC in range 0.1-0.5 % (phr)	1.1055-1.2586
AZDC in range 1-7 % (phr)	0.9006-1.0078

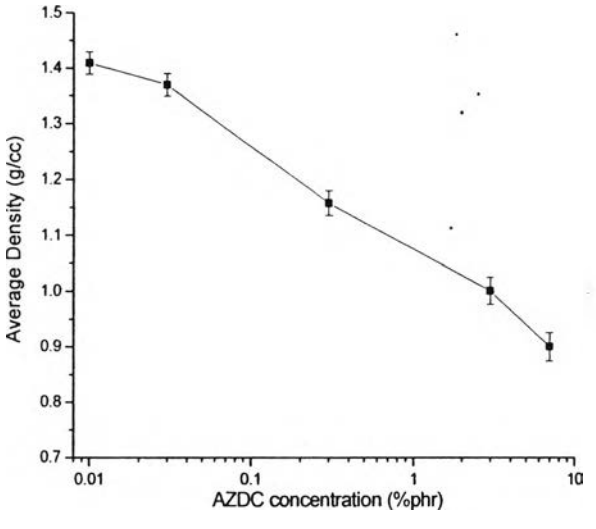

Figure 5.7 The densities of porous PVDF in different AZDC concentrations (phr).

The density of the resulting foam depends on the concentration of AZDC solids in PVDF. The density of unfilled, solid PVDF is around 1.7894 g/cc. This process can yield minimum to maximum foam densities of 0.9006-1.4093 g/cc. Figure 5.7 shows AZDC 7% with a lowest density, due to their more bubbles inside structure.

5.4.3 Pore Diameter of Porous films

The average pore sizes of porous PVDF films can be determined by using program SemAfore 5.00 JEOL.

Table 5.2 Average pore diameter of PVDF with AZDC in different fraction (phr)

Sample	Average pore diameter (μm)
PVDF with AZDC 0.03% (phr)	56.39 (Min.30.45, Max.120.77)
PVDF with AZDC 0.3% (phr)	82.42 (Min.42.95, Max.135.02)
PVDF with AZDC 3% (phr)	146.90 (Min.135,Max.198.89)

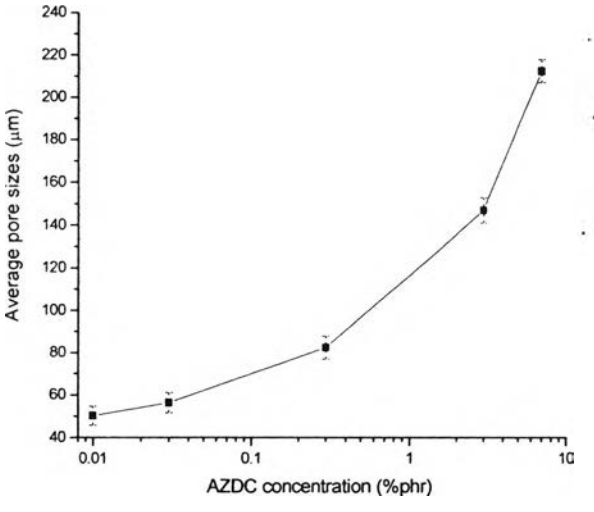

Figure 5.8 Average pore sizes of porous PVDF films in different AZDC fractions.

A clear effect of AZDC concentrations (phr) on cell size was observed in Figure 5.8. As concentration of AZDC (phr) increased, so was the viscosity of PVDF in the melt state, leading to lower resistance in the cell growth stage. It can be noted that the average cell size was found to increase with increasing AZDC.

5.4.4 Porosity Measurement of PVDF films

The porous PVDF films were immersed in iso-butanol around 24 hr then taken them out to remove iso-butanol on the surface before weighing and calculating the porosity that available in the literature [Minghao Gu. Gu *et al.* (2006)].

Table 5.3 Porosity of porous PVDF films by different solvent (thickness 120 μm)

Sample	Average % Porosity
AZDC 0.01-0.05% (phr)	43.62-44.99
AZDC 0.1-0.5% (phr)	49.57-55.88
AZDC 1-7% (phr)	65.43-73.56

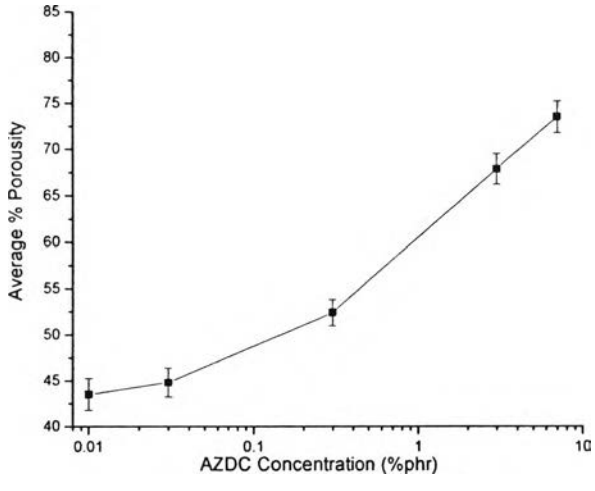

Figure 5.9 The effect of AZDC concentration (phr) on % porosity.

The volume fraction of voids in the PVDF foam can be up to 73.56%. In general, increasing the AZDC content increases the foam cell size. It can be implied that the larger the average bubbles diameters, the more % porosity or foam cell volumes as shown in Figure 5.9.

5.4.5 Thermal Properties Analysis-TGA

The thermal decomposition of microporous PVDF films with different blowing agent concentrations and porosity percentages can be determined by TG-DTA.

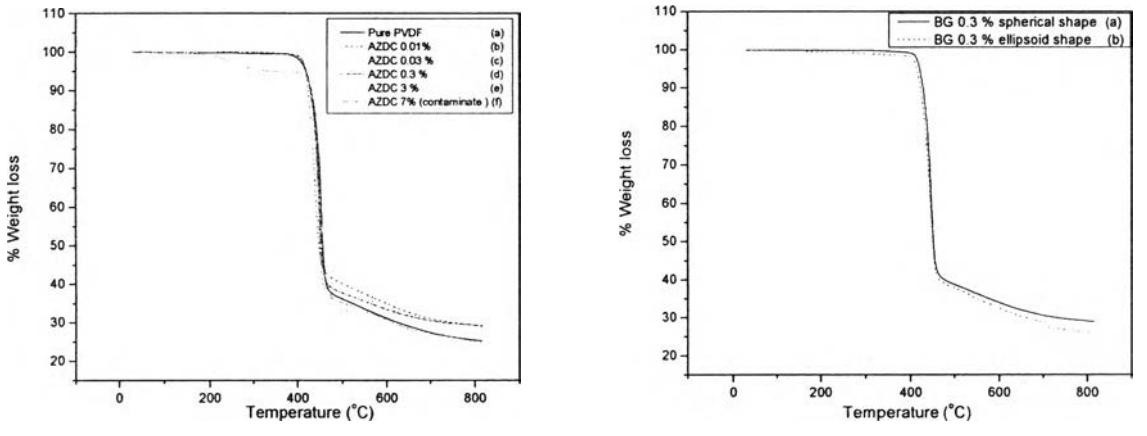

(a) **(b)**

Figure 5.10 TGA thermograms of PVDF films in different (a) % BG and (b) shape of bubble

In Figure 5.10 shows the TGA graphs of weight loss versus temperature for PVDF and internal bubbles. The degradation of porous PVDF is similar in range 447.98-448.94°C same as phase inversion results. From all TG-DTA results, it can be suggested that the decomposition temperature (T_d) of porous PVDF films not depend on the amount of air penetrated, type of porous structure, and stretching.

5.4.6 Melting behavior -DSC

The DSC graphs of endothermic consumes T_m show the amount of air and stretching does not influence in the melting temperature of PVDF/air composites because of no interactions or chemical bonding with polymer matrix as reveals in Figure 5.7.

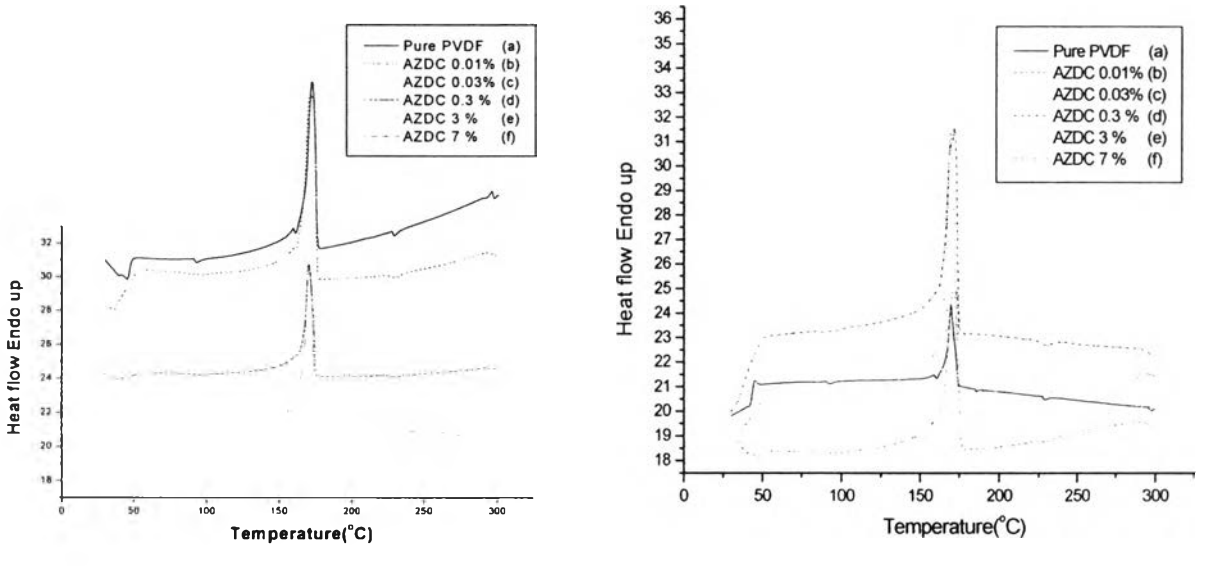

Figure 5.11 DSC graphs of porous PVDF films in different (a) mount of air and (b) shapes.

The crystallinity was calculated and shown that the nonporous PVDF film is 51 % and porous PVDF films from different AZDC concentration nearly the same to 50.74-51.53 % as shown in Figure 5.11 (a). In Figure 4.16 (b) shows crystallinity slightly increases with draw ratio increases which crystalline of the unstretched nonporous PVDF film is abruptly increases up to 64.79 %. For porous PVDF films by AZDC compression molding were slightly increased to 56.67- 57.21 % due to stretched PVDF films have higher orientation than non-stretched PVDF films. As results, the porous PVDF from compression molding is lower crystallinites than phase inversion.

5.4.7 β-phase analysis-XRD

The crystallinity and percentage of β-phase data were exactly measured by XRD (WAXD). In Figure 5.12 shows XRD profiles of non-stretching and stretching of flat PVDF films, the peaks in 2θ Bragg angle with values of 20°and 27° corresponding to the plane [(1 1 0),(0 2 1)] that corresponds to α-phase. After the samples were stretched (1:1 ratio) under force, the overlapping of (111) and (201) were exhibited at 37°. From this XRD pattern can be calculated %F(β) of non-stretching is 21.36% and stretching is

strongly increase to 71.65 %, due to the β-phase is increased, whereas overlapping of (111) and (021) 27° theta azimuthally angle reflections of α-phase disappear according to Mohammadi, B., Yousefi, A.A., Bellah, S. M. (2007). As can be seen in Figure 5.12, all porous PVDF films exhibited a similar diffraction pattern. The curve fitting of amorphous and crystalline region in XRD can be calculated crystallinites of porous films to 20.83-21.58 % by varying amount of air. For the stretching film can be seen in Figure 5.12 (b) the diffraction angles of WAXD at 27° that corresponds to α is missing whereas the diffraction angles at near 37° that correspond to the β phase are present [Campos, J.S.C., Ribeiro, A.A., Cardoso, C.X. (2007)]. The effect of stretching porous PVDF films on %β crystallites that occurred in 31.45-35.5%. The %β crystallinity is strongly improved by stretching in case of flat PVDF film. On the other hand, the porous PVDF slightly increased (Calculated for all on these angle ranges).

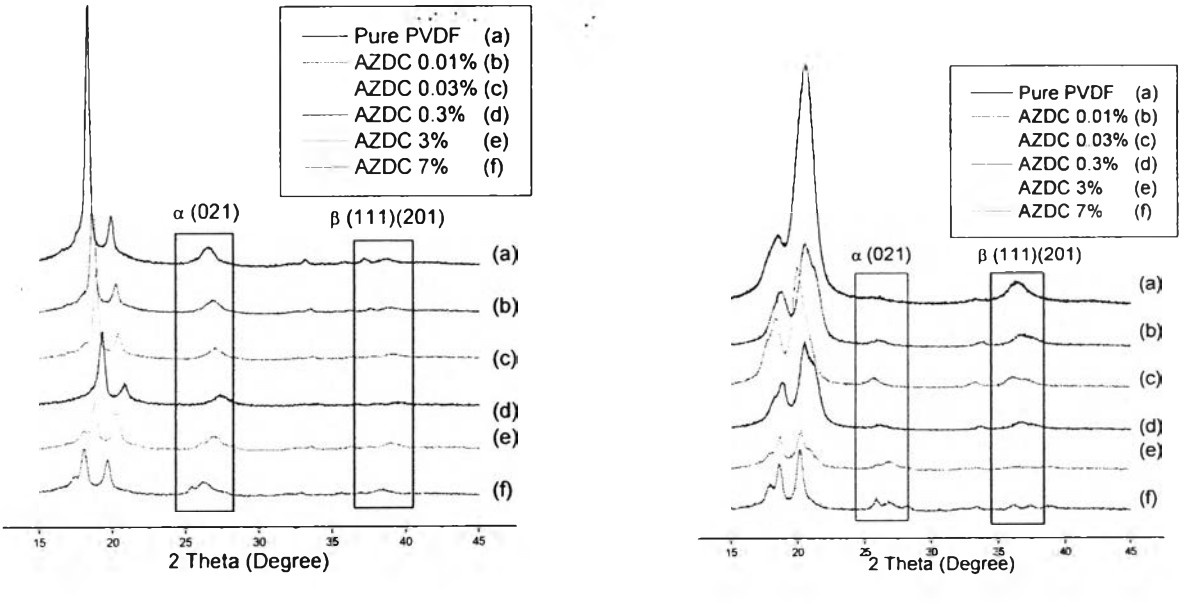

Figure 5.12 XRD diffractograms of porous PVDF films: (a) spherical and (b) ellipsoid shapes with different % AZDC or amount of air.

B. Electrical Properties

5.4.8 Dielectric Behavior -LCR meter

a) Effect concentration of AZDC 0.01, 0.03, 0.3, 3,and 7 (%phr)

The dielectric properties of the PVDF films with various air fractions measured as a function of frequency range of 100 Hz -10 MHz are shown in Fig 5.13. It shows that the highest dielectric constant is 11 obtained from ellipsoidal shape.

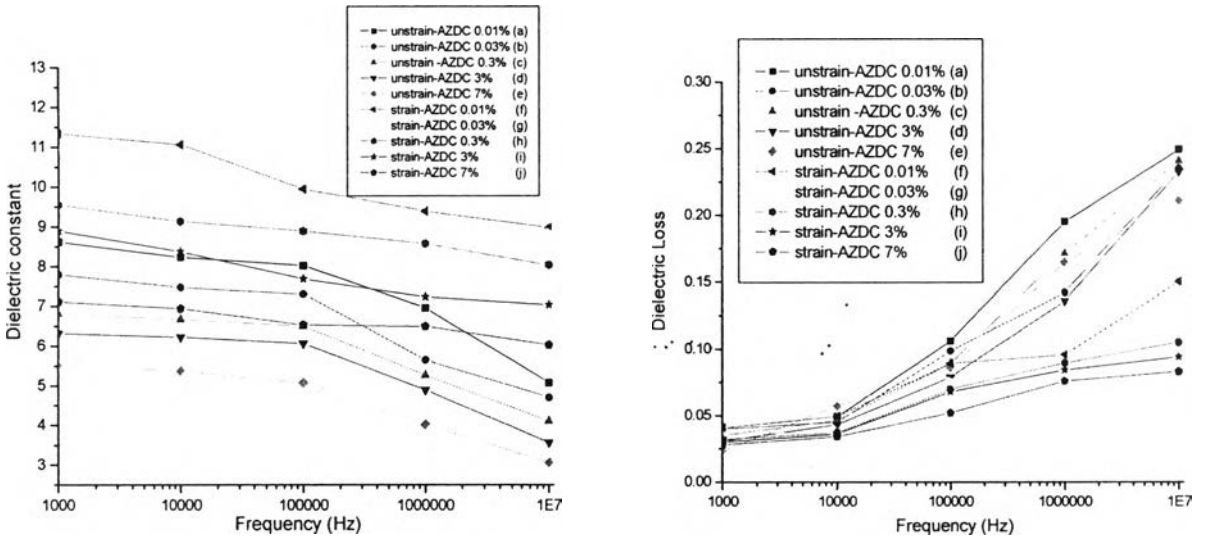

(a) **(b)**

Figure 5.13 The frequency dependence of the (a) dielectric constant and (b) dielectric loss tangent with frequency at room T ° of porous PVDF films by compression molding at in different % weight of AZDC and different shape.

Figure 5.13 can be implied that the value of dielectric constant increases with decreasing AZDC concentration from 7 to 0.01% (phr) of PVDF/Air ratio, due to the fact that the pores behave as a mixture of air which have dielectric constant of 1. Also, the dielectric loss decrease with increasing amount of air bubbles which can be seen that 7% AZDC for ellipsoidal shape shows lower loss tangent than 0.01% at various frequencies. Also, all shape and air content of porous films are lower than 0.25 at frequency up to10 MHz.

b) Effect of shape (spherical and ellipsoidal)

For spherical shape, their dielectric constant values dropped rapidly at high frequency (> 1 MHz) and loss tangent increased abruptly. This phenomenon was due to spherical can be occurred more dipolar relaxation than ellipsoidal shape. The comparison of dielectric constant in spherical and ellipsoidal shapes is shown in Figure 5.14. The dielectric constants of spherical bubbles PVDF films are lower than those of ellipsoid for all bubbles PVDF films compositions. This is related to the electric displacement generated in the ellipsoidal shape. Moreover, the ellipsoidal shape has wider air gap and higher surface area than spherical shape.

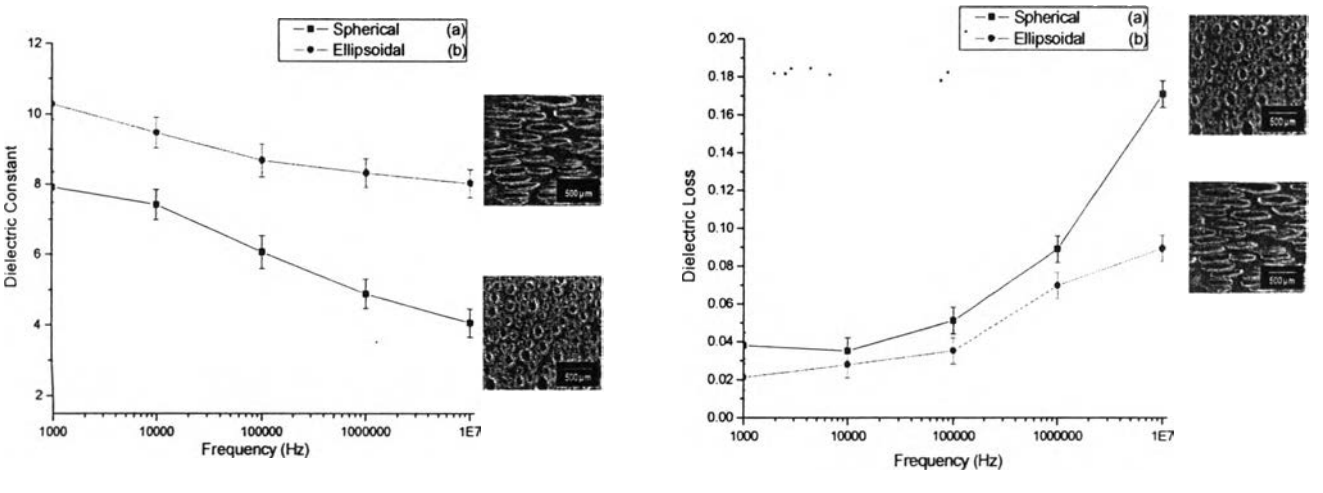

(a) **(b)**

Figure 5.14 Frequency dependent (a) dielectric constant and (b) dielectric loss of porous PVDF films with different shape between spherical and ellipsoidal shape.

c) Effect of bubbles distribution (cellular and non-cellular)

In Figure 5.15 show dielectric and loss tangent between cellular (phase inversion) and non-cellular in the same porosity or amount of air. This phenomenon could be explained that cellular exhibits large dielectric relaxation at frequency greater

than 1 MHz (dipolar relaxation). The decrease in the dielectric constant was due to the delay in molecular polarization with respect to a changing frequency in polymer.

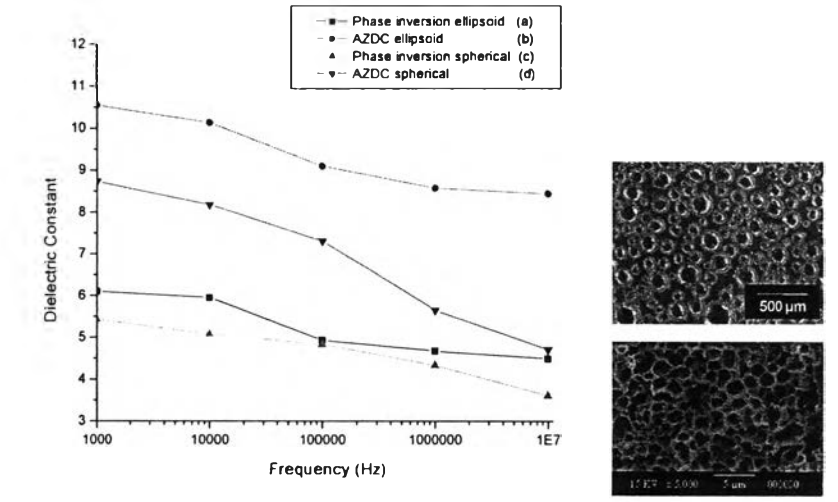

(a)

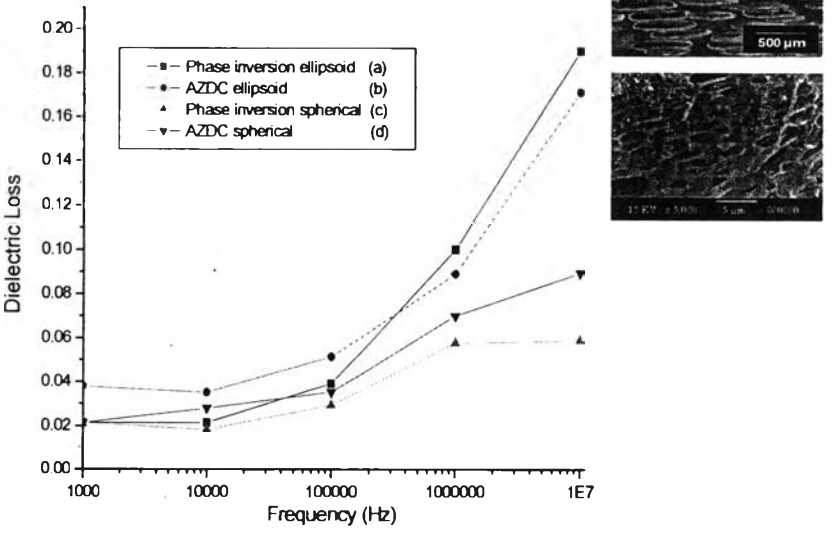

(b)

Figure 5.15 Comparing (a) dielectric properties and (b) dielectric loss of phase inversion and blowing agent techniques.

As seen from Figure 5.15, the non- cellular structure (blowing agent) have a higher the dielectric constant than cellular structure (phase inversion) due to porous

PVDF films from phase inversion technique have a lower thin wall of bubbles and polymer concentrations (chance to occurred β-phase) than blowing agent technique. A lower loss is also obtained when the diameter of a microbubble and air gap bubble decreases.

5.4.9 0-3 connectivity of Air Bubbles/PVDF composites-curve fitting

As already discussed from previous work, a composite with 0-3 connectivity consists of bubbles connected in zero dimensions and a three dimensionally interconnected PVDF matrix. The theoretical mixing models including Yamada model, Bruggeman formulae, Lichtenecker model, and Kerner expression modified by Jayasundere-Smith (J-S prediction) have been fitted with the dielectric constant from experimental results.

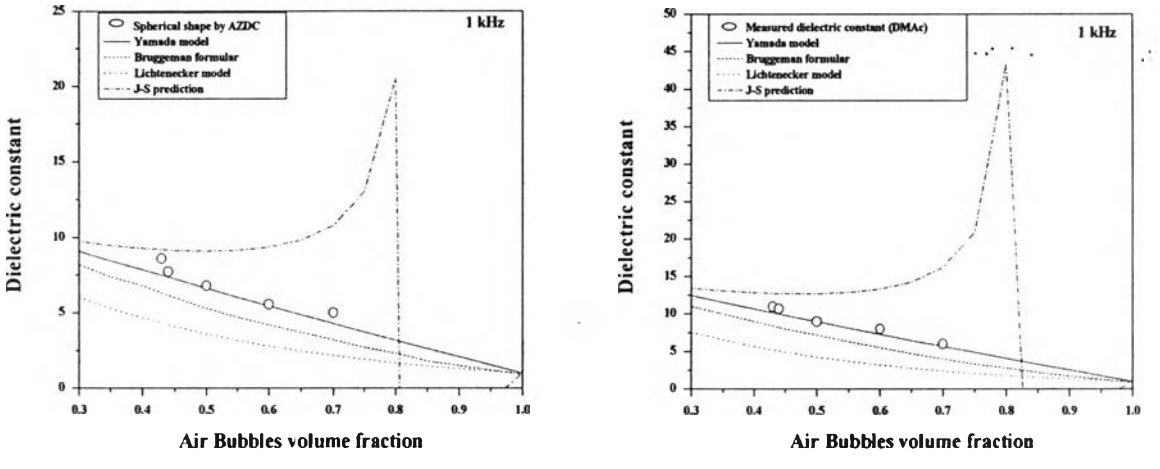

Figure 5.16 Plot of theoretical models and the measured dielectric constant of (a) spherical and (b) ellipsoidal shape in different air volume fractions at room temperature and 1 kHz.

In Figure 5.16, the measured dielectric constants of the porous PVDF by AZDC compression molding are agree slightly well with the theoretical prediction based on Yamada model indicating 0-3 connectivity. For Bruggeman formula, J-S prediction and

Lichtenecker model was lower than the measured dielectric constants. Among these theoretical models, the measured dielectric constants fit well with Yamada model.

5.5 Conclusion

The non-cellular regular spherical bubble shape of PVDF films were produced by azodicabonamide (AZDC) chemical blowing agent technique. The increasing concentration of AZDC (phr) in PVDF powder can yield a higher pore size, porosity and density. This result can be explained by the agglomeration of fine particles and increase to larger particle as a higher % AZDC. From TGA thermograms result, it was found that internal bubble not effect on a decomposition temperature and a stretching PVDF film (ellipsoidal shape) has no effect on melting temperature but stretching are slightly effects on β-phase crystallinity of PVDF film which confirmed by XRD diffraction. However, dielectric properties of non-cellular were higher than those of the cellular structure (from phase inversion) but considerably low when compared with the pure PVDF films (non-porous). Surprisingly, an ellipsoidal bubble shape can be enhanced dielectric properties than spherical shape in porous PVDF films. The reason can be explained that ellipsoidal shape was created the electric displacement in bubbles and their have lower air gap like an electrode in side PVDF films. And also, these ellipsoidal shapes have stable loss tangent in the frequency range of 1 kHz to 10 MHz which indicated the low relaxation behavior. Finally, Yamada model could fit the measured dielectric constant well for all composites indicating 0-3 connectivity that very interesting properties for piezoelectric lightweight applications.

5.6 Acknowledgements

The authors wish to thank MTEC staffs as electronic measurement for useful assistance and instrument for characterizations. The partial funding of research work was provided by the National Excellence Center for Petroleum, Petrochemicals, and Advanced Materials, Thailand.

5.7 Reference

Afifuddin, S. (1996) An Investigation of Fundamental Properties of Very Thin Ferroelectric Polymer Films. Master Thesis. School of Mathematics, Physics, Computing and Electronics. Macquarie University, Sydney, NSW, Australia.

Chan, H.L.W. and Unsworth, J. (1989) Simple model for piezoelectric ceramic polymer 1-3 composites used in ultrasonic transducer applications, IEEE Trans. Ultrason., Ferroelec, Freq. Contr., 36 : 434- 441.

Campos, J.S.C., Ribeiro, A.A., Cardoso, C.X. (2007) Preparation of characterization of PVDF/$CaCO_3$ composites. Journal of Materials Science& Engineering B, 136, pp 123-128

C. Zeped a Sahagun and R. Gonzalec-Nunez (2006) Morphology of Extruded PP/HDPE Foam Blends Journal of cellular plastics Volume 42 — November.

Das-Gupta, D.K. (1994) Ferrooelectric Polymers and Ceramic Polymer Composites. Trans Tech Publ, Zurich.

Dias, C.J., and Das-Gupta, D.K. (1996) Ferroelectric ceramic/polymer composite electric, IEEE Trans. on Dielectric and Material Insul, 3 : 706-711.

Di Maio, E., Mensitieri, G., Iannace, S., Nicolais, L., Li, W. and Flumerfelt, R.W. (2005) Structure Optimization of Polycaprolactone Foams by using Mixture of CO2 and N2 as Blowing Agent, Polymer Engineering and Science, 45(7): 432–441.

Gibson, L.J. and Ashby, M.F. (1988). Cellular Solids: Structure and Properties, Pergamon Press, Oxford.

H. Kawai. (1969), The piezoelectricity of poly(vinyledene fluoride), Jpn. J. Appl .Phys. 8, 975.

H.S. Nalwa.(1991) Recent developments in ferroelectric polymers, Macromol. Chem. Phys. (Rev.) C31 (4) (1991) 341.

Ikeda, T. (1990) Fundamental of piezoelectricity, Oxford Science Publications, New York.

John Murphy,(1996) Additives for plastics, hand book, Elseviser Science Ltd., 177-187.

Kawai, H. (1969) The Piezoelectricity of Polyvinylidene Fluoride, Jpn.J. Appl. Phys.,8 :975-976.

Klempner, D. and Sendijarevic, V. (2004) Polymeric Foams and Foam Technology, Hanser Gardner, Munich.

Park, C.P.(1991) *Handbook of Polymeric Foams and Foams Technology*, 375. Hanser Publisher, Munich.

R.C. Patil, S. Radhakrishnan, S. Pethkar, K. Vijayamohanan. (2001) Piezoresistivity of conducting polyaniline/BaTiO3 composites, J. Mater. Res. 16 (7) 1982.

S.B. Lang. (1993) Guide to the literature of piezoelectricity and pyroelectricity, Ferroelectrics 139 (1993) 141.

Van der Vegt, N.F.A., Briels, W.J., Wessling, M. and Strathmann, H. (1999) The Sorption Induced Glass Transition in Amorphous Glassy Polymers, Journal of Chemical Physics, 110(22): 11061–11069.